ACS APPLIED MATERIALS & INTERFACES

Research Article

www.acsami.org

Fabrication of a Detection Platform with Boronic-Acid-Containing Zwitterionic Polymer Brush

Lingjie Song,[†,‡] Jie Zhao,[†] Shifang Luan,*[,†] Jiao Ma,[†] Jingchuan Liu,[†] Xiaodong Xu,[§] and Jinghua Yin*[,†]

[†]State Key Laboratory of Polymer Physics and Chemistry, Changchun Institute of Applied Chemistry, Chinese Academy of Sciences, Changchun 130022, P. R. China

[‡]University of Chinese Academy of Sciences, Beijing 100049, P. R. China

[§]Polymer Materials Research Center and Key Laboratory of Superlight Materials & Surface Technology, Ministry of Education, College of Materials Science and Chemical Engineering, Harbin Engineering University, Harbin 150001, P. R. China

Supporting Information

ABSTRACT: Development of technologies for biomedical detection platform is critical to meet the global challenges of various disease diagnoses, especially for point-of-use applications. Because of its natural simplicity, effectiveness, and easy repeatability, random covalent-binding technique is widely adopted in antibody immobilization. However, its antigen-binding capacity is relatively low when compared to site-specific immobilization of antibody. Herein, we report that a detection platform modified with boronic acid (BA)-containing sulfobetaine-based polymer brush. Mainly because of the advantage of oriented immobilization of antibody endowed with BA-containing three-dimensional polymer brush architecture, the platform had a high antigen-binding capacity. Notably, nonspecific protein adsorption was also suppressed by the zwitterionic pendants, thus greatly enhanced signal-to-noise (S/N) values for antigen recognition. Furthermore, antibodies captured by BA pendants could be released in dissociation media. This new platform is promising for potential applications in immunoassays.

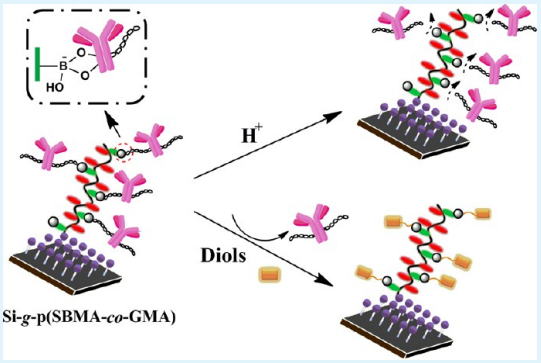

KEYWORDS: *atom transfer radical polymerization (ATRP), zwitterionic-based materilals, boronic acid (BA), antibody immobilization, immunoassay*

1. INTRODUCTION

Over the past decades, developing biosensors with high sensitivity and detection efficiency has been the focus of research interest because of its tremendous role in predicting diseases.[1−7] For achieving specific recognition of a target biomolecule with high-sensitivity, a proper strategy for antibody immobilization is a vital key to success.[8] Antibody immobilization manner greatly affects antibody−antigen interactions on an assay support, which is an essential process for the development of immune-based assay systems.[9] Compared with physical adsorption, covalent antibody binding has many advantages such as stability, effectiveness and easy repeatability. Especially for site-specific immobilization of antibodies, their antigen-binding capacity is usually 2-3 folds larger than that of the randomly-coupled ones.[10−14] Various oriented antibody coupling approaches have been proposed for obtaining high analyte feedback signal.[15−19] The site-specific antibody immobilization by taking advantage of Fc constant region is more preferable because it can achieve homogeneous surface coverage and guarantee available accessibility to the antigen-binding epitopes. In one scheme, Fc receptors, such as protein A or protein G, are widespreadly used to bind the Fc portion of antibody. Nevertheless, a drawback of such receptors mediated immobilization is lack of enough control on the orientation of themselves. Another strategy relies on the chemical or enzymic oxidation of carbohydrate moieties located at Fc region. However, the requisite treatments on antibody are very likely to trigger the possibility of reduction, even loss of bioactivity.[20,21] Therefore, new strategies that present proper and uniform orientation, minimum antibody modification and soft incubation conditions, are urgently needed.[22]

Complex formation of boronic acids (BAs) with mono- and oligosaccharides in aqueous solutions is well known for many years.[23] This virtue makes BAs widely used in the detection of adenosine,[24] saccharide,[25−28] sialic acid,[29] as well as controllable cell immobilization.[30−33] Furthermore, the BA-containing materials (BCMs) are capable of recognizing and separating glycoprotein.[34−38] It has been confirmed by Ivanov et al. that because of a large number of the pendant groups in the chains, BCMs can interact with their biological receptors in a multivalent way, enhancing the affinity and specificity of biomimetic binding.[39,40] However, up to now, just a few works

Received: September 25, 2013
Accepted: December 4, 2013
Published: December 4, 2013

 © 2013 American Chemical Society

focusing on oriented immobilization of antibodies through boronate formation for immunoassays have been reported.[41,42]

Meanwhile, because of the fact that the abundant proteins exist in plasma or body fluid, the unavoidable nonspecific protein adsorption on biosensor surface is another real challenge which need to be overcome in order to maintain high antigen recognition efficiency and suppress false noisy.[43] Hence, the inhibition of nonspecific protein adsorption is usually accomplished by the implementation of surface modification with highly hydrophilic polymer brushes on a support.[44−46] The poly(ethylene oxide) (PEG)-based materials have excellent anti-fouling properties;[47−50] however, their auto-oxidization in aqueous solution, especially in the existence of transitionmetal ions, compromises their long-term protein-repellent capability.[51] Recently, particular attention has been paid to the zwitterionic-based materials with high resistance to protein adsorption, such as phosphorylcholine (PC),[52,53] carboxybetaine (CB),[54,55] and sulfobetaine (SB).[56] Jiang et al. reported a series of zwitterionic CB-based platforms with single-layer or controlled hierarchical structures via "grafting from" methods. The large grafting density of CB and three-dimensional polymer brush architecture imparted the ultra-low fouling and high protein loading properties even in human blood plasma, thereby providing potential applications for biosensors.[57,58]

Herein, we demonstrated a detection platform modified with BA-containing zwitterionic polymer brush that provided both the oriented antibodies immobilization and low nonspecific protein adsorption (Scheme 1). First, the substrate was grafted with polymer brushes consisting of SB and glycidyl methacrylate (GMA) by using surface-initiated atom transfer radical polymerization (SI-ATRP). Second, aminophenyl boronic acid (APBA) introduced through the reaction of epoxy pendant and amino group acts as a specific capture site for oriented immobilization of antibody. Simultaneously, the hydrophilic SB zwitterionic polymer brushes can satisfy the needs of suppression nonspecific protein adsorption and be conductive to the retention of antibody bioactivity. Protein adsorption, bioassay, and antibody dissociation were systematically investigated using a confocal laser scanner.

Scheme 1. Schematic Representation of Preparing BA-Containing Zwitterionic Polymer-Brush-Modified Platform for Antibody Immobilization and Antigen Detection

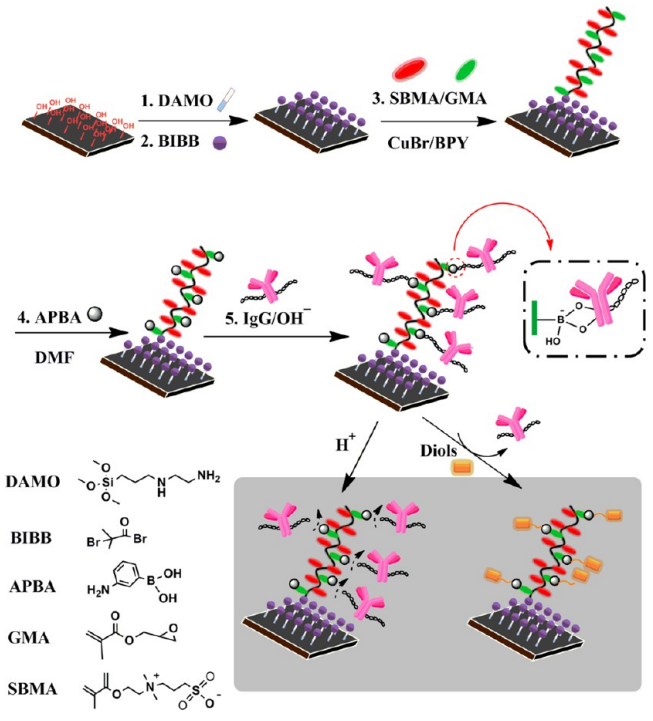

2. EXPERIMENTAL SECTION

Materials. 3-[Dimethyl-[2-(2-methylprop-2-enoyloxy) ethyl] azaniumyl] propane-1-sulfonate (SBMA), Glycidyl methacrylate (GMA), 3-Aminophenylboronic acid (APBA), Copper(I) bromide (CuBr), 2-bromopropionyl-bromide (BIBB), 3-Glycidoxypropyl-trimethoxysilane (GPTMS) and Trihydroxymethyl aminomethane (Tris) were purchased from Sigma-Aldrich. [3-(2-Aminoethyl) aminopropyl] trimethoxysilane (DAMO) was provided by Acros. 2,2′-Bipyridine (Bpy) was purchased from Alfa-Aesar. Toluene, dichloromethane (DCM), triethylamine (TEA), and dimethyl formamide (DMF), dextran, glucose, and sorbitol were purchased from Haodi Company. Phosphate buffered saline (PBS, pH 7.2) was supplied by Dingguo Biology. All proteins with or without fluorescence labeled (fluorescein isothiocyanate (FITC) or Rhodamin B isothiocyanate (RBITC)) including bovine serum albumin (BSA), goat to rabbit IgG (Go-to-Ra IgG), rabbit IgG, mouse to goat IgG (Mo-to-Go IgG) were all provided by Bioss Biotechnology. GMA was passed through a basic alumina column to remove inhibitors. Solvents such as DCM, TEA, and toluene were immediately subjected to distillation in the presence of drying agent (calcium hydride for DCM and TEA, sodium/benzophenone for toluene) before use. Other reagents was AR grade and used as received.

Preparation of Functionalized Polymer-Brush-Modified Wafers. After treated by freshly prepared piranha solution (30 vol. % H_2O_2 and concentrated H_2SO_4, 1:3 (v/v)), the silicon wafers (1 cm × 2 cm) were placed into an anhydrous toluene solution containing DAMO or GPTMS (2 vol %) at room temperature for 2 h to get resultant products which were denoted as Si-DAMO or Si-GPTMS. The Si-DAMO was immersed into anhydrous DCM solution containing TEA (10 vol %) in ice/water bath for 30 min, followed by dropwise addition of BIBB solution (10 vol %) in DCM overnight, and was then cleaned and dried to get the resulting wafer (denoted as Si-DAMO-BIBB). The pSBMA brush-based surfaces were prepared as follows. A piece of Si-DAMO-BIBB wafer, CuBr (1 mmol), and $CuBr_2$ (0.2 mmol) were placed into a three-neck flask under nitrogen protection. Then, SBMA (7 mmol) and Bpy (2 mmol) were predissolved in a 12 mL DI water/methanol (1/1, v/v) mixture, purged with Ar gas for 30 min and transferred to the flask. The graft-polymerization reaction was conducted under Ar atmosphere at 40 °C for 6 h. After being washed with methanol and ultrapure water, the resultant wafer is acquired (referred to as Si-*g*-pSBMA). Similar to the above SI-ATRP procedures, the pGMA, p(SBMA-*co*-GMA)$_{1:1}$, and p(SBMA-*co*-GMA)$_{10:1}$ brush-based surfaces were fabricated. The 1/5 volume ratio of DI water/methano mixture was used for the pGMA-modified sample preparation.

APBA Binding and Oriented Immobilization of Primary Antibody. Binding APBA was easily realized by the reaction between epoxy groups from pGMA brush or GPTMS and amine groups from APBA. The details were listed as follows: the as-prepared samples were first soaked in 10 mL of APBA-contained DMF solution (20 mg/mL) under stirring at 50 °C for 24 h, and transferred into ethanolamine solution (0.5 M) for 2 h to quench the residual epoxy groups. After being rinsed with water and ethanol, the APBA-modified wafers were finally obtained (referred to as Si-*g*-pGMA-APBA, Si-*g*-p(SBMA-*co*-GMA)$_{1:1}$-APBA, Si-*g*-p(SBMA-*co*-GMA)$_{10:1}$-APBA, and Si-GPTMS-APBA, respectively).

After 2 h incubation in Tris-HCl solution (2 mM, pH 9), these samples were soaked in Tris-HCl solutions containing Go-to-Ra IgG primary antibody (10, 20, 50, 100, 200, and 500 ng/mL) at 4 °C for 24 h, followed by rinsing with Tris-HCl solution and ultrapure water to remove physisorbed IgG. The resultant samples were denoted as Si-*g*-

pGMA-APBA-IgG, Si-*g*-p(SBMA-co-GMA)$_{1:1}$-APBA-IgG, Si-*g*-p-(SBMA-*co*-GMA)$_{10:1}$-APBA-IgG, and Si-GPTMS-APBA-IgG, respectively.

Evaluation of Primary Antibody Immobilization, Antigen Recognition, and S/N Value. Amount of immobilized primary antibody was evaluated as the following procedures. The IgG-immobilized samples were blocked with BSA and dextran solution (1 mg/mL) at room temperature for 1 h, and then incubated in PBS solution containing Mo-to-Go IgG-FITC secondary antibody (20 μg/mL) at 4 °C for 24 h, followed by rinsing, drying, and examining by fluorescence intensity scanning.

For rabbit IgG antigen recognition, the specific IgG-immobilized surface was first prepared by using Go-to-Ra IgG solution (20 μg/mL), rinsed with Tris-HCl buffer and ultrapure water, and then incubated in FITC-labeled rabbit IgG antigen solution (from 1 pg/mL to 1 μg/mL, PBS) at 4 °C for 24 h. After the physisorbed antigen was removed by PBS solution and ultrapure water, the samples were tested by fluorescence intensity scanning.

For the evaluation of signal-to-noise (S/N) value, the whole procedures were similar to the above antigen recognition, except that the incubation solution was prepared by different concentration of FITC-labeled target antigen (1 pg/mL, 10 pg/mL, 10 ng/mL, and 1 μg/mL) and RBITC-tagged BSA (200 μg/mL).

Primary Antibody Dissociation. Dissociation processes of the Go-to-Ra IgG primary antibody immobilized by APBA were conducted in different pH and sugar solutions. The IgG-immobilized surfaces were prepared at a 20 μg/mL concentration of FITC-labeled Go-to-Ra IgG solution as mentioned before, followed by washing with PBS solution containing Tween-20 (5 %, w/v) to remove the physical adsorbed protein, and dried under an Ar stream. The samples were incubated in different pH dissociation solutions (Citrate-phosphate buffer (pH 3) and Tris-HCl buffer (pH 9) containing sugars (Flu and Glu) for a desired time. The as-prepared samples were washed with PBST solution and ultrapure water, and finally examined by the following fluorescence intensity scanning.

Nonspecific Protein Adsorption Evaluation. To evaluate the nonspecific protein adsorption resistance, the samples were first incubated in PBS solution for 2 h, then soaked in PBS solution containing FITC-labeled BSA (200 μg/mL) at 4 °C for 12 h, rinsed, dried, and finally examined by fluorescence intensity scanning.

Surface Chemical Composition. Surface elemental compositions of the samples were determined via X-ray photoelectron spectroscopy with Al/Kα ($h\nu$ = 1486.6 eV) anode mono-X-ray source (XPS, VG Scientific ESCA MK II Thermo Avantage V 3.20 analyzer) at the detection angle of 90o. Spectra over a range of 0-1200 eV, and high-resolution spectra of C_{1s}, N_{1s}, O_{1s}, B_{1s}, Br_{3d}, and S_{2p} regions were collected. Atomic concentrations of the elements were calculated by their corresponding peak areas.

Surface Wettability. Water static contact angles on the surfaces were measured with a drop shape analysis instrument (DSA, KRÜSS GMBH, Hamburg 100) at room temperature. For each sample, a 2 μL water droplet was dropped each time and at least five contact angle measurements were performed for calculating the average value.

Surface Morphology. Surface morphology of the samples was examined by an atomic force microscopy (AFM) with contact mode (SPA300HV with a SPI 3800 controller, Seiko Instruments Industry, Japan). The root-mean-square (RMS) roughness was evaluated directly from AFM images.

Fluorescence Intensity Scanning and Data Analysis. Fluorescent images of the samples were collected by a confocal laser scanning microscope (Zeiss, LSM 700). Target biomolecules labeled with FITC and RBITC were respectively excited by an argon ion laser at 488 nm and 555 nm. To obtain fluorescence intensity, we analyzed the original fluorescent images using Image Pro software. Fluorescence intensity value was measured from six different positions of each fluorescence image.

3. RESULTS AND DISCUSSION

Surface Characterization. XPS data confirmed that the sequence procedures of initiator binding, SI-ATRP polymerization and APBA immobilization (Figure 1, Table 1). In Figure 1, the strong peak of N (9.95 %) suggested the formation of self-assemble DAMO monolayer (Figure 1b). The anchoring of BIBB was indicated by peak of Br (1.67 %) (Figure 1c). After 6 h ATRP polymerization, grafting copolymer brushes were confirmed by substantial increases in C and S signals (Figure 1d–g). When these surfaces were functionalized with APBA, the typical B signal could be detected. Decreasing molar ratio of GMA in copolymer, the amount of immobilized APBA also decreased, along with the varied [B]/[C] values from 79.52 to 65.13 to 39.03%. To fully examine the different chemical groups presented on these surfaces, we analyzed high-resolution of N_{1s}, O_{1s}, and C_{1s} spectra (Figures S1–S3 in the Supporting Information). The high-resolution C_{1s} spectra were curve-fitted into following chemical functional groups: O–C=O (288.8 eV), C–O–C (286.9 eV), C–N (286.4 eV), C–S (285.6 eV), C–C/C–H (284.6 eV), and C–B (283.8 eV). In high-resolution O_{1s} spectra, a series of functional groups containing O=C–O (533.7 eV), O=C–O (532.2 eV), C–O–C/C–O (533.1 eV), S=O (531.8 eV), S–O (532.5 eV), and B–O (531.5 eV) were presented. Meanwhile, the B–O/O=C–O ratio values, representing the percentage of introduced APBA amount relative to the total content of copolymer, were

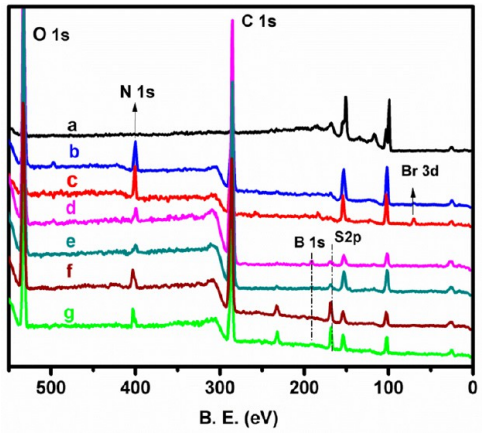

Figure 1. XPS spectra of the samples. (a) Virgin Si wafer, (b) Si-DAMO, (c) Si-DAMO-BIBB, (d) Si-*g*-pGMA-APBA, (e) Si-*g*-p(SBMA-*co*-GMA)$_{1:1}$-APBA, (f) Si-*g*-p(SBMA-*co*-GMA)$_{10:1}$-APBA, (g) Si-*g*-pSBMA.

Table 1. XPS Atomic Concentrations of the Samples

	XPS atomic concentration (at %)						
sample[a]	[C]	[O]	[S]	[N]	[B]	[Br]	[B]/[C]
a	13.92	30.15					
b	36.74	27.29	0.89	9.95		0.31	
c	36.55	25.12	1.03	13.44		1.67	
d	54.02	29.45	0.62	5.62	3.93	0.32	7.28
e	52.57	27.71	1.36	2.96	3.53	0.34	6.71
f	49.55	23.06	4.39	5.08	2.43	0.17	4.90
g	62.66	24.95	5.00	4.72		0.31	

[a](a) virgin Si wafer, (b) Si-DAMO, (c) Si-DAMO-BIBB, (d) Si-*g*-pGMA-APBA, (e) Si-*g*-p(SBMA-*co*-GMA)$_{1:1}$-APBA, (f) Si-*g*-p(SBMA-*co*-GMA)$_{10:1}$-APBA, (g) Si-*g*-pSBMA.

decreased from 79.52 to 65.13 to 39.03% with increasing the molar ratio of [SBMA]/[GMA] from 0:1 to 1:1 to 10:1. In high-resolution N_{1s} spectra, the peak areas variation of the chemical groups of −NH (399.8 eV), $-NH_3^+$ (402.5 eV), and corresponding B_{1s} (191.6 eV) also suggested that the contents of pSBMA and pGMA in copolymer were correlated to the dosage ratio of [SBMA]/[GMA] monomers, and the amount of the immobilized APBA was well-dependent on the content of pGMA in copolymer brushes.

As shown in wettability test (Figure 2), varied water contact angle (WCA) values were observed following the correspond-

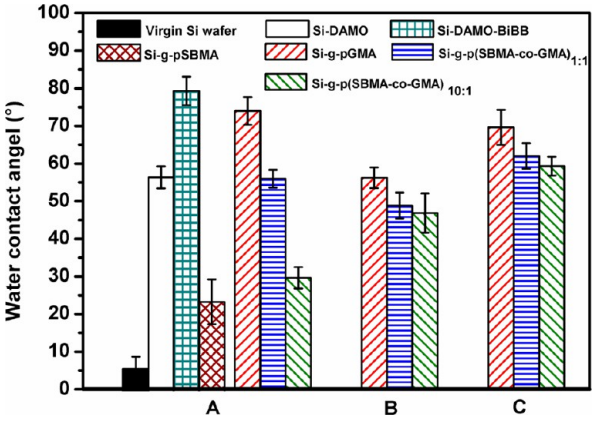

Figure 2. Water contact angle of the samples after surface modifications of (A) initiator immobilization and SI-ATRP polymerization, (B) APBA binding, (C) IgG loading. (The error bars: standard deviations, n = 5).

ing surface modifications. It increased from ∼10° for fresh silicon substrate to ∼55° for Si-DAMO and ∼80° for Si-DAMO-BIBB because of the successive reduction in the hydrophilicity of fresh silicon, DAMO and BIBB. As for the surfaces modified with polymer brushes, due to the electrostatically induced hydration, the pSBMA-modified surface (∼28°) showed the lowest WCA value. Further increasing the content of less hydrophilic pGMA segments resulted in a gradually increased tendency in WCA values (∼74°, for pGMA-modified substrate). The hydrophilicity of APBA, IgG, and pGMA-containing substrates have a little difference, thus the WCA values varied accordingly. Figure 3 showed the surface morphologies of polymer brush-modified and antibody-immobilized samples. Low roughnesses (RMS values: 2.2, 3.2, and 2.8 nm, respectively) were observed on the polymer brush-modified surfaces, suggesting the uniform and controlled polymer brushes were prepared by the controlled SI-ATRP technique. In contrast, the additional immobilization of IgG molecules to the polymer brush modified surfaces exhibited granular structures in the AFM images and much larger roughness.[59] These granules in size and roughness decreased widely as the pGMA fraction increased because the IgG layer is more compact for the higher IgG loading.[60]

Nonspecific Protein Adsorption. Evaluation of protein-repellent properties was conducted after antibody attachment on the supports. The samples were allowed to incubate in PBS buffer containing FITC-BSA model protein and the amount of BSA adsorbed on the supports were indirectly exhibited by the fluorescence intensities.[61,62] As shown in Figure 4, Si-*g*-pGMA-APBA-IgG exhibited the highest fluorescence intensity (∼110 K), which is nearly 2 times higher than that of control sample (∼50 K). The introduction of pSBMA brushes can effectively alleviate protein adsorption behaviors: ∼55 K intensity value for Si-*g*-p(SBMA-*co*-GMA)$_{1:1}$-APBA-IgG and ∼10 K for Si-*g*-p(SBMA-*co*-GMA)$_{10:1}$-APBA-IgG, and negligible protein adsorption for Si-*g*-pSBMA, primarily because of the hydrated layer formed on the surface via electrostatic interaction between zwitterionic pSBMA brushes and water molecules.

Capacities of Primary Antibody Immobilization. Herein, we used FITC-labeled second antibody to determine the amount of immobilized primary antibody. As shown in Figure 5, the stronger fluorescence signal was detected on the Si-GPTMS-APBA-IgG surface with respect to the Si-GPTMS-IgG reference, probably because site-specific immobilization of antibody via BA pendants guaranteed that antigen-binding sites were effectively exposed in media.[23,41] Notably, the antibody loading on the supports modified with BA-containing polymer brushes, even for Si-*g*-p(SBMA-*co*-GMA)$_{10:1}$-ABPA-IgG with the lowest content of GMA, was 2−3 orders of magnitude larger than Si-GPTMS-APBA-IgG reference. The GPTMS self-assembled monolayer provided less number of active sites to bind antibodies due to the occurrence of a single layer of epoxy groups. However, formation of the polymer brush on the surface via the SI-ATRP led to a sharp increase in epoxy group number, thereby enhancing the amount of bound antibody. Besides, other factors such as steric hindrance caused by the neighbouring antibody and distance between the bound antibody and support also could be weakened and eliminated by constructing the flexible polymer-brush-formed surfaces. In the group of polymer-brush-modified surfaces, as pGMA fraction in polymer brush decreased, antibody loading of the samples was reduced regardless of primary antibody concentrations.

A high content of SBMA can effectively resist nonspecific protein adsorption, whereas sufficient content of GMA can offer more active sites to bind APBA. Therefore, an optimal ratio between these two functional monomers is needed to endow the surface with high protein adsorption resistance and enough active sites for future antibody-antigen interaction. For this reason, different monomer ratios of SBMA and GMA were adopted in our experiment. It was confirmed that the sample with a ratio of SBMA/GMA at 10:1 was ideal.

Target Antigen and Signal-to-Noise (S/N) Value Evaluation. Binding capacity of antigen is mainly correlated to the antibody loading, antibody bioactivity and antibody orientation, etc.[9] For the as-prepared detection platform, target recognition was benefited from SI-ATRP for several reasons: First, enhanced antibody loading capacity was obtained. Second, it is well-recognized that direct immobilization of antibodies on a solid substrate often influences the antigen recognition as a result of steric hindrance and limited mobility of bound antibody. Thus, a long and flexible linker could be utilized for more frequent antibody-antigen binding.[22,63−66] In our system, the graft chains not only served the same purpose as the long and flexible linke but also inhibited hydrophobic interactions between native substrate and antibody due to the existence of zwitterionic pendants. Third, a 3D space distribution of antibody in the polymer brush might promote the collision probability between antibody and free antigen in medium relative to a 2D layer structure. More importantly, the oriented immobilization of antibodies by the BA pendants further facilitated the maximum accessibility of antigens to bioactive epitopes on antibodies. As discussed above, the supports modified with BA-containing polymer brush had high

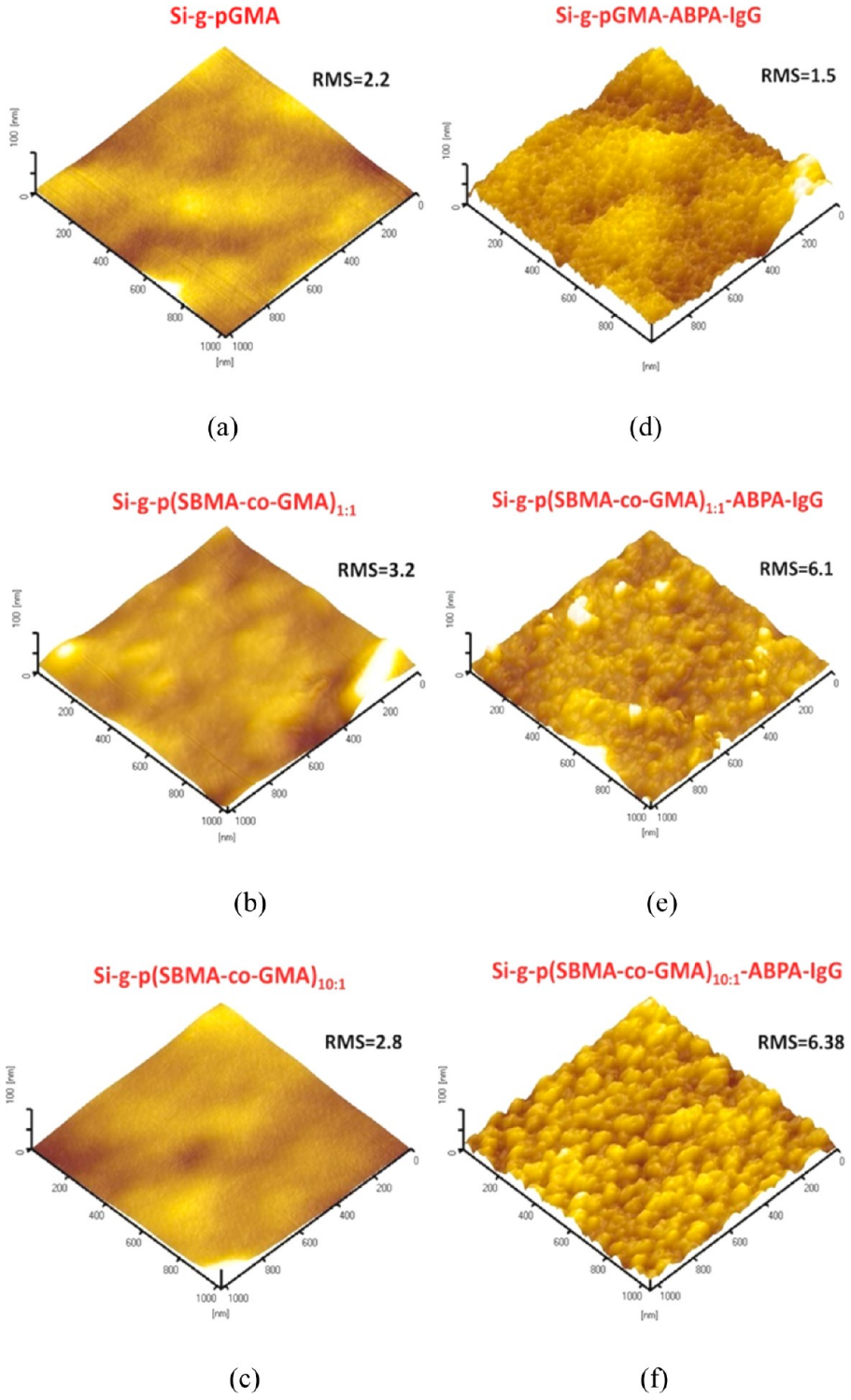

Figure 3. AFM three-dimensional topogrophic images of the samples. (a) Si-*g*-pGMA, (b) Si-*g*-p(SBMA-*co*-GMA)$_{1:1}$, (c) Si-*g*-p(SBMA-*co*-GMA)$_{10:1}$, (d) Si-*g*-pGMA-APBA-IgG, (e) Si-*g*-p(SBMA-*co*-GMA)$_{1:1}$-APBA-IgG, (f) Si-*g*-p(SBMA-*co*-GMA)$_{10:1}$-APBA-IgG. (1μm × 1μm scanning area.).

detection efficiencies with the antigen concentrations ranging from 1 pg/mL to 1 μg/mL (Figure 6). The samples with lower content of epoxy pendants generally have relatively smaller antibody loading, but the difference of antibody loading among these samples was almost negligible at lower antigen concentrations. This means epoxy content will rarely affect diagnosis performances because target analyte concentrations are extremely low in clinic diagnosis.

To detect a specific disease marker in practice, we usually conducted the biosensors in the complicated crude blood or body fluid media. The undesired adsorption of nonspecific components (noise) seriously hindered and interfered the specific detection of analyte (signal), resulting in a low detection sensitivity. On the basis of this understanding, two model components, FITC-labeled target antigen and RBITC-tagged BSA, were adopted and tried to investigate the

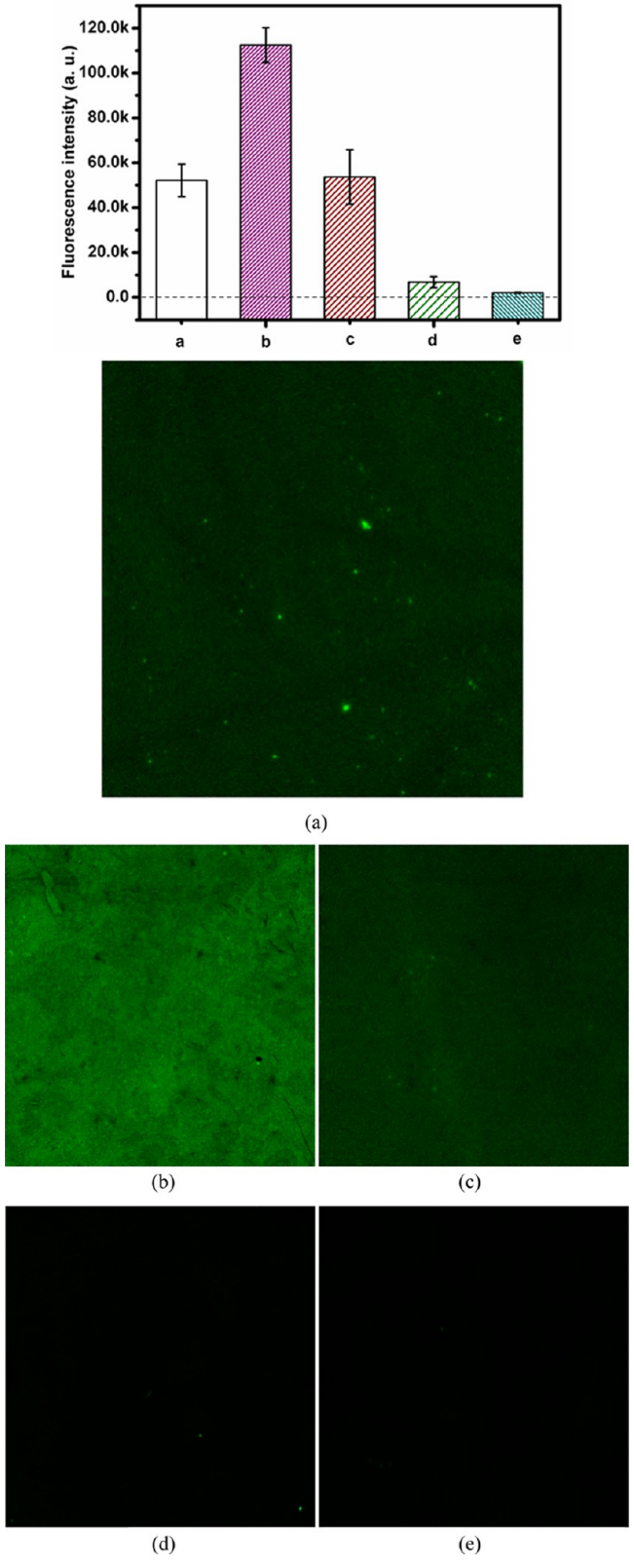

Figure 4. Fluorescence intensity and representative fluorescence images of FITC -BSA protein adsorption on the surfaces. (a) virgin Si wafer, (b) Si-*g*-pGMA-APBA-IgG, (c) Si-*g*-p(SBMA-*co*-GMA)$_{1:1}$-APBA-IgG, (d) Si-*g*-p(SBMA-*co*-GMA)$_{10:1}$-APBA-IgG, and (e) Si-*g*-pSBMA. (The error bars: standard deviations, n = 6).

relationship between signal and noise on the functionalized surfaces via the confocal laser scanning microscope. Herein, the detection platforms were incubated in the mixture protein solution of the FITC-labeled target antigen and RBITC-tagged BSA, then two different fluorescence signals from the analyte and interference were separately collected and their fluorescence intensity ratios (defined as S/N value) were calculated (Figure 7A). As for Si-*g*-pGMA-APBA-IgG, although S/N values slightly rose from ∼1 to ∼3 with increasing antigen concentration, fluorescence intensities of noises were comparable to that of the target analyte. The correct extraction of analyte signal was greatly affected by the strong nonspecific protein adsorption. In contrast, the S/N values were largely enhanced after the introduction of pSBMA brushes, and increasing pSBMA contents makes a continual increased tendency of S/N value. The Si-*g*-p(SBMA-*co*-GMA)$_{10:1}$-APBA-IgG sample had the highest S/N values (∼20), which was 6 times larger than that of the Si-*g*-pGMA-APBA-IgG reference. In Figure 7B, fluorescence images of the samples incubated in PBS solution containing FITC-labeled target antigen (1pg/mL) and RBITC-tagged BSA (200 μg/mL) were choosed as representatives. We could visually observe that overlay image from the Si-*g*-p(SBMA-*co*-GMA)$_{10:1}$-APBA-IgG sample was total green, whereas the other samples presented orange-green color, especially for Si-*g*-pGMA-APBA-IgG. These results demonstrated that the ability of surface nonspecific protein resistance adsorption was obviously enhanced by increasing the pSBMA fraction, thus presenting favorable results including the low noise, the minimal possibility of false information, and improved sensitivity for target detection.

Antibody Dissociation. As widely reported, the BA-containing substrates possessed the smart, reversible, and reusable properties because the interactions between BA and diols are pH-responsive.[64] Similarly, the as-prepared BA-containing platforms would provide potential applications in renewable biosensors, except for their advantage of site-selectively capture of antibody. In this test, antibody dissociation behaviors under different pH and saccharide molecule competitor were examined. From the reduction in fluorescence intensities after antibody dissociation, it revealed that the conjunction between boronic acid and glycosyl had been disrupted in acid solution (pH 3) (Figure 8). However, the calculated dissociation efficiencies from fluorescence intensities (generally lower than 50 %) were below expectation. To investigate this phenomenon, fluorescence-labeled BSA adsortpions on pSBMA-modified surfaces were conducted at pH 3, 7, and 9 in buffer soutions (see Figure S5 in the Supporting Information). We found that the amount of the adsorbed BSA in acid solution were repectively ∼5 and ∼3 times higher than that in neutral and alkaline solution, suggesting that the acid condition compromised the anti-fouling capability of pSBMA brush. It was mainly reponsible for the low antibody dissociation efficiencies calculated from fluorescence intensities. Actually, dissociation efficiencies should be relatively higher.

Because of the fact that alkaline environment just slightly affected the anti-fouling capability of pSBMA-modified supports, antibody dissociation experiments were conducted under alkaline environment in the presence of sorbitol and glucose which were powerful and appropriate eluent agents for the regeneration of BA-based sensing system. Sorbitol dissociation media presented high dissociation efficiencies with values ranging from ∼54% to ∼82%, whereas those for glucose dissociation media were generally less than ∼63% (∼45

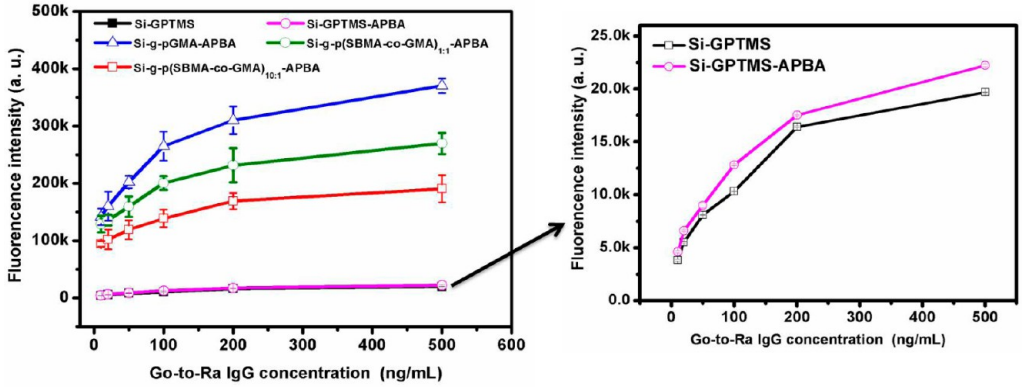

Figure 5. Fluorescence intensity evaluation of antibody loading. (The error bars: standard deviations, n = 6).

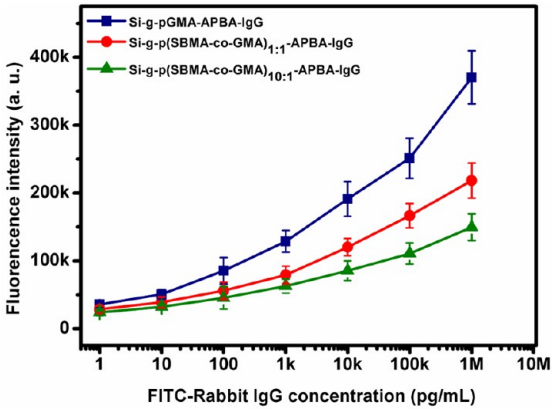

Figure 6. Fluorescence intensity of the IgG-immobilized supports after rabbit IgG antigen recognition. (The error bars: standard deviations, n = 6).

to ~63%). In these procedures, the antibody dissociation efficiency of Si-*g*-p(SBMA-*co*-GMA)$_{10:1}$-APBA-IgG sample reached up to ~82% as compared with the highest value of ~56% for Si-*g*-PGMA-APBA-IgG sample (Figure 8, Figure S6 in the Supporting Information). The lower dissociation efficiency on pure pGMA-modified surface was due to the strong physisorption of glycoproteins, which already examined by the FITC-BSA adsorption test. This also suggested that zwitterionic pendants played an essential role in favor of the antibody dissoicaition under alkaline environment.

4. CONCLUSIONS

We have demonstrated a platform modified with polymer brushes consisting of BA and zwitterionic SB for immunodiagnostic detection. Antibody loadings on the as-prepared platform were 2−3 orders of magnitude larger than GPTMS references. Mainly due to site-specific immobilization of antibody via 3D BA-containing polymer brush, an efficient antigen detection platform was obtained. Nonspecific protein adsorption was effectively inhibited by the presence of zwitterionic pendants in polymer brush. Furthermore, their signal-to-noise (S/N) ratios in antigen recognition were increased by ~6 times relative to Si-*g*-pGMA-APBA-IgG references, presenting a high sensitivity towards target analyte. In addition, antibodies captured by BA can be released by adjusting pH of medium, species of saccharide. Our strategy for surface modification of detection platform is also applicable to the fabrication of other biosensors.

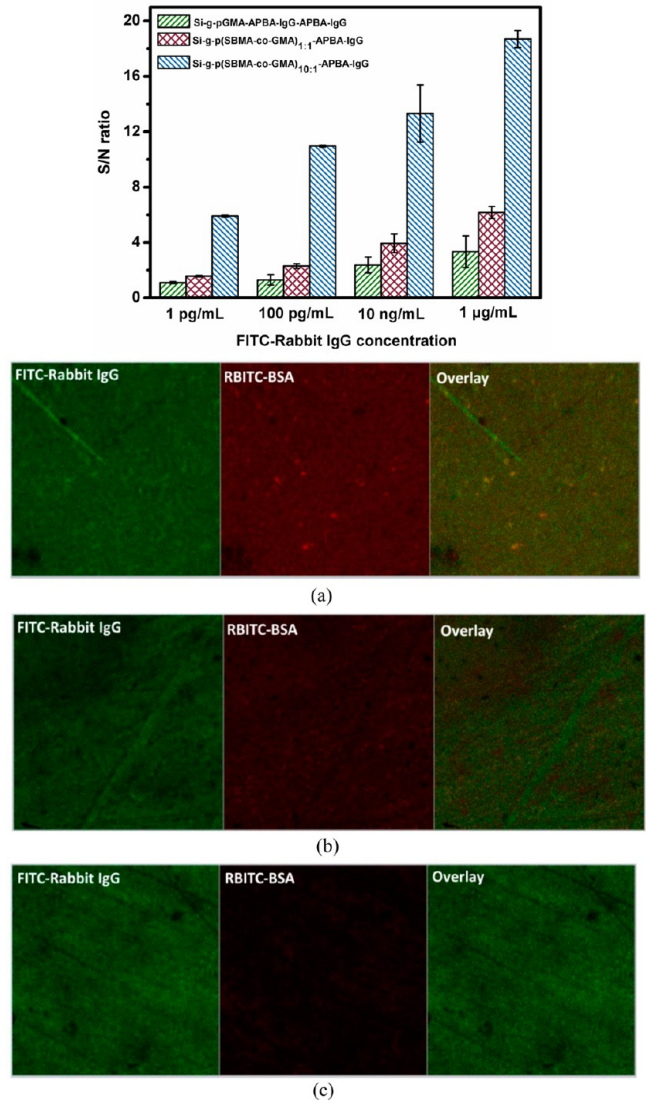

Figure 7. S/N ratio values and representative fluorescence images of antigen detection in the presence of BSA interference. (a)Si-*g*-pGMA-APBA-IgG, (b) Si-*g*-p(SBMA-*co*-GMA)$_{1:1}$-APBA-IgG, (c) Si-*g*-p-(SBMA-*co*-GMA)$_{10:1}$-APBA-IgG. (The error bars: standard deviations, n = 3).

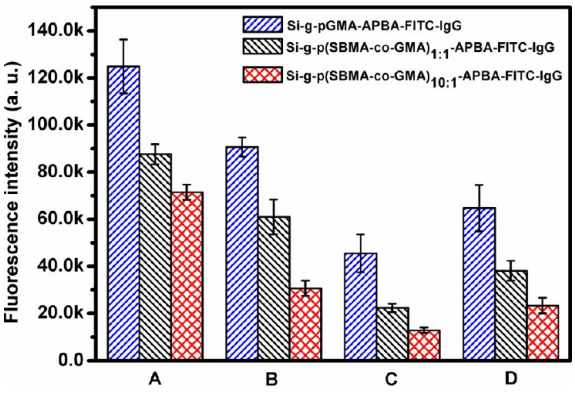

Figure 8. Fluorescence intensities of the FITC-IgG immobilized samples. (A) and antibody dissociation under condition of (B) pH 3, 6 h; (C) pH 9, sorbitol 200 mM, 6 h; (D) pH 9, glucose 200 mM, 6 h (error bars: standard deviations, n = 6).

■ ASSOCIATED CONTENT

Supporting Information

Details of chemical group compositions in high-resolution O_{1s}, N1s and C 1s spectra of the samples; Fluorescence intensities of FITC-BSA protein adsorption on samples without and with IgG immobilization; fluorescence intensities of FITC-BSA protein adsorption on Si-*g*-pSBMA sample under different pH environments; fluorescence intensities of FITC-IgG dissociation under different sorbitol conditions. This material is available free of charge via the Internet at http://pubs.acs.org/.

■ AUTHOR INFORMATION

Corresponding Authors

*Tel.: +86 431 85262109. Fax: +86 431 85262109. E-mail: yinjh@ciac.ac.cn.

*E-mail: sfluan@ciac.ac.cn

Notes

The authors declare no competing financial interest.

■ ACKNOWLEDGMENTS

The authors acknowledge the financial support of the National Science Foundation of China (Projects 21274150, 51273200, and 51103030), Chinese Academy of Sciences-Wego Group High-tech Research & Development Program (2011-2013), and Scientific Development Program of Jilin Province (Project 20130102064JC). The uthors gratefully acknowledge the assistance of Senior Engineer Yongxian Song in the State Key Laboratory of Polymer Physics and Chemistry, Changchun Institute of Applied Chemistry.

■ REFERENCES

(1) Deng, W. P.; Xu, B.; Hu, H. Y.; Li, J. Y.; Hu, W.; Song, S. P.; Feng, Z.; Fan, C. H. *Sci. Rep.* **2013**, *3*, 1−6.

(2) Tian, J. F.; Jarujamrus, P.; Li, L. Z.; Li, M. S.; Shen, W. *ACS Appl. Mater. Interfaces* **2012**, *4*, 6573−6578.

(3) Zhang, J.; Wang, L. H.; Zhang, H.; Boey, F.; Song, S. P.; Fan, C. H. *Small* **2010**, *6*, 201−204.

(4) Gubala, V.; Harris, L. F.; Ricco, A. J.; Tan, M. X.; Williams, D. E. *Anal. Chem.* **2012**, *84*, 487−515.

(5) Song, S. P.; Qin, Y.; He, Y.; Huang, Q.; Fan, C. H.; Chen, H. Y. *Chem. Soc. Rev.* **2010**, *39*, 4234−4243.

(6) Cheng, K.; Blumen, S. R.; MacPherson, M. B.; Steinbacher, J. L.; Mossman, B. T.; Landry, C. C. *ACS Appl. Mater. Interfaces* **2010**, *2*, 2489−2495.

(7) Li, J.; Song, S. P.; Liu, X. F.; Wang, L. H.; Pan, D.; Huang, Q.; Zhao, Y.; Fan, C. H. *Adv. Mater.* **2008**, *20*, 497−500.

(8) Gubala, V.; Gandhiraman, R. P.; Volcke, C.; Doyle, C.; Coyle, C.; James, B.; Daniels, S.; Williams, D. E. *Analyst* **2010**, *135*, 1375−1381.

(9) Trilling, A. K.; Beekwilder, J.; Zuilhof, H. *Analyst* **2013**, *138*, 1619−1627.

(10) Gubala, V.; Crean, C.; Nooney, R.; Hearty, S.; McDonnell, B.; Heydon, K.; O'Kennedy, R.; MacCraith, B. D.; Williams, D. E. *Analyst* **2011**, *136*, 2533−2541.

(11) Laib, S.; MacCraith, B. D. *Anal. Chem.* **2007**, *79*, 6264−6270.

(12) Grazu, V.; Abian, O.; Mateo, C.; Batista-Viera, F.; Fernández-Lafuente, R.; Guisán, J. M. *Biomacromolecules* **2003**, *4*, 1495−1501.

(13) Gubala, V.; Le Guevel, X.; Nooney, R.; Williams, D. E.; MacCraith, B. *Talanta* **2010**, *81*, 1833−1839.

(14) Lu, B.; Smyth, M. R.; OKennedy, R. *Analyst* **1996**, *121*, R29−R32.

(15) Trilling, A. K.; Harmsen, M. M.; Ruigrok, V. J. B.; Zuilhof, H.; Beekwilder, J. *Biosens. Bioelectron.* **2013**, *40*, 219−226.

(16) Hu, X. J.; Hortiguela, M. J.; Robin, S.; Lin, H.; Li, Y. J.; Moran, A. P.; Wang, W. X.; Wall, J. G. *Biomacromolecules* **2013**, *14*, 153−159.

(17) Alves, N. J.; Kiziltepe, T.; Bilgicer, B. *Langmuir* **2012**, *28*, 9640−9648.

(18) Seo, M. H.; Han, J.; Jin, Z.; Lee, D. W.; Park, H. S.; Kim, H. S. *Anal. Chem.* **2011**, *83*, 2841−2845.

(19) Batalla, P.; Fuentes, M.; Grazu, V.; Mateo, C.; Fernandez-Lafuente, R.; Guisan, J. M. *Biomacromolecules* **2008**, *9*, 719−723.

(20) Kang, J. H.; Choi, H. J.; Hwang, S. Y.; Han, S. H.; Jeon, J. Y.; Lee, E. K. *J. Chromatogr. A* **2007**, *1161*, 9−14.

(21) Karyakin, A. A.; Presnova, G. V.; Rubtsova, M. Y.; Egorov, A. M. *Anal. Chem.* **2000**, *72*, 3805−3811.

(22) Jung, Y. W.; Jeong, J. Y.; Chung, B. H. *Analyst* **2008**, *133*, 697−701.

(23) Chen, M. L.; Adak, A. K.; Yeh, N. C.; Yang, W. B.; Chuang, Y. J.; Wong, C. H.; Hwang, K. C.; Hwu, J. R. R.; Hsieh, S. L.; Lin, C. C. *Angew. Chem., Int. Ed.* **2008**, *47*, 8627−8630.

(24) Ivanov, A. E.; Galaev, I. Y.; Mattiasson, B. *Macromol. Biosci.* **2005**, *5*, 795−800.

(25) Matsumoto, A.; Ikeda, S.; Harada, A.; Kataoka, K. *Biomacromolecules* **2003**, *4*, 1410−1416.

(26) Shoji, E.; Freund, M. S. *J. Am. Chem. Soc.* **2002**, *124*, 12486−12493.

(27) James, T. D.; Sandanayake, K. R. A. S.; Shinkai, S. *Nature* **1995**, *374*, 345−347.

(28) Matsumoto, A.; Yoshida, R.; Kataoka, K. *Biomacromolecules* **2004**, *5*, 1038−1045.

(29) Matsumoto, A.; Sato, N.; Kataoka, K.; Miyahara, Y. *J. Am. Chem. Soc.* **2009**, *131*, 12022−12023.

(30) Ivanov, A. E.; Panahi, H. A.; Kuzimenkova, M. V.; Nilsson, L.; Bergenstahl, B.; Waqif, H. S.; Jahanshahi, M.; Galaev, I. Y.; Mattiasson, B. *Chem.—Eur. J* **2006**, *12*, 7204−7214.

(31) Liu, H. L.; Li, Y. Y.; Sun, K.; Fan, J. B.; Zhang, P. C.; Meng, J. X.; Wang, S. T.; Jiang, L. *J. Am. Chem. Soc.* **2013**, *135*, 7603−7609.

(32) Ivanov, A. E.; Kumar, A.; Nilsang, S.; Aguilar, M. R.; Mikhalovska, L. I.; Savina, I. N.; Nilsson, L.; Scheblykin, I. G.; Kuzimenkova, M. V.; Galaev, I. Y. *Colloids Surf., B* **2010**, *75*, 510−519.

(33) Ivanov, A. E.; Eccles, J.; Panahi, H. A.; Kumar, A.; Kuzimenkova, M. V.; Nilsson, L.; Bergenstahl, B.; Long, N.; Phillips, G. J.; Mikhalovsky, S. V.; Galaev, I. Y.; Mattiasson, B. *J. Biomed. Mater. Res. A* **2009**, *88A*, 213−225.

(34) Liu, Y. C.; Ren, L. B.; Liu, Z. *Chem. Commun.* **2011**, *47*, 5067−5069.

(35) Zhou, W.; Yao, N.; Yao, G. P.; Deng, C. H.; Zhang, X. M.; Yang, P. Y. *Chem. Commun.* **2008**, 5577−5579.

(36) Bicker, K. L.; Sun, J.; Lavigne, J. J.; Thompson, P. R. *ACS Comb. Sci.* **2011**, *13*, 232−243.

(37) Hjertén, S.; Li, J. P. *J. Chromatogr. A* **1990**, *500*, 543−553.

(38) Liu, X. C.; Scouten, W. H. *J. Mol. Recognit.* **1996**, *9*, 462−467.

(39) Ivanov, A. E.; Solodukhina, N.; Wahlgren, M.; Nilsson, L.; Vikhrov, A. A.; Nikitin, M. P.; Orlov, A. V.; Nikitin, P. I.;

Kuzimenkova, M. V.; Zubov, V. P. *Macromol. Biosci.* **2011**, *11*, 275−284.
(40) Ivanov, A. E.; Shiomori, K.; Kawano, Y.; Galaev, I. Y.; Mattiasson, B. *Biomacromolecules* **2006**, *7*, 1017−1024.
(41) Ho, J. A. A.; Hsu, W. L.; Liao, W. C.; Chiu, J. K.; Chen, M. L.; Chang, H. C.; Li, C. C. *Biosens. Bioelectron.* **2010**, *26*, 1021−1027.
(42) Lin, P. C.; Chen, S. H.; Wang, K. Y.; Chen, M. L.; Adak, A. K.; Hwu, J. R. R.; Chen, Y. J.; Lin, C. C. *Anal. Chem.* **2009**, *81*, 8774−8782.
(43) Huang, C. J.; Brault, N. D.; Li, Y.; Yu, Q.; Jiang, S. *Adv. Mater.* **2012**, *24*, 1834−1837.
(44) Källrot, M.; Edlund, U.; Albertsson, A. C. *Biomaterials* **2006**, *27*, 1788−1796.
(45) Kyomoto, M.; Ishihara, K. *ACS Appl. Mater. Interfaces* **2009**, *1*, 537−542.
(46) Edlund, U.; Källrot, M.; Albertsson, A.C. *J. Am. Chem. Soc.* **2005**, *127*, 8865−8871.
(47) Xiu, K. M.; Cai, Q.; Li, J. S.; Yang, X. P.; Yang, W. T.; Xu, F. J. *Colloids Surf., B* **2012**, *90*, 177−183.
(48) Chen, H.; Wang, L.; Zhang, Y. X.; Li, D.; McClung, W. G.; Brook, M. A.; Sheardown, H.; Brash, J. L. *Macromol. Biosci.* **2008**, *8*, 863−870.
(49) Xu, F. J.; Li, H. Z.; Li, J.; Eric Teo, Y. H.; Zhu, C. X.; Kang, E. T.; Neoh, K. G. *Biosens. Bioelectron.* **2008**, *24*, 773−780.
(50) Xu, F. J.; Liu, L. Y.; Yang, W. T.; Kang, E. T.; Neoh, K. G. *Biomacromolecules* **2009**, *10*, 1665−1674.
(51) Gao, C.; Li, G.; Xue, H.; Yang, W.; Zhang, F.; Jiang, S. *Biomaterials* **2010**, *31*, 1486−1492.
(52) Matsuda, Y.; Kobayashi, M.; Annaka, M.; Ishihara, K.; Takahara, A. *Langmuir* **2008**, *24*, 8772−8778.
(53) Yuan, B.; Chen, Q.; Ding, W. Q.; Liu, P. S.; Wu, S. S.; Lin, S. C.; Shen, J.; Gai, Y. *ACS Appl. Mater. Interfaces* **2012**, *4*, 4031−4039.
(54) Vaisocherová, H.; Zhang, Z.; Yang, W.; Cao, Z.; Cheng, G.; Taylor, A. D.; Piliarik, M.; Homola, J.; Jiang, S. *Biosens. Bioelectron.* **2009**, *24*, 1924−1930.
(55) Zhao, J.; Song, L. J.; Shi, Q.; Luan, S. F.; Yin, J. H. *ACS Appl. Mater. Interfaces* **2013**, *5*, 5260−5268.
(56) Kuo, W. H.; Wang, M. J.; Chien, H. W.; Wei, T. C.; Lee, C.; Tsai, W. B. *Biomacromolecules* **2011**, *12*, 1348−4356.
(57) Jiang, S.; Cao, Z. *Adv. Mater.* **2010**, *22*, 920−932.
(58) Vaisocherová, H.; Yang, W.; Zhang, Z.; Cao, Z.; Cheng, G.; Piliarik, M.; Homola, J. i.; Jiang, S. *Anal. Chem.* **2008**, *80*, 7894−7901.
(59) Kim, J.; Cho, J.; Seidler, P. M.; Kurland, N. E.; Yadavalli, V. K. *Langmuir* **2010**, *26*, 2599−2608.
(60) You, H. X.; Lowe, C. R. *J. Colloid Interf. Sci.* **1996**, *182*, 586−601.
(61) Goli, K. K.; Rojas, O. J.; Genzer, J. *Biomacromolecules* **2012**, *13*, 3769−3779.
(62) Zhang, N.; Pompe, T.; Amin, I.; Luxenhofer, R.; Werner, C.; Jordan, R. *Macromol. Biosci.* **2012**, *12*, 926−936.
(63) Raj, J.; Herzog, G.; Manning, M.; Volcke, C.; MacCraith, B. D.; Ballantyne, S.; Thompson, M.; Arrigan, D. W. M. *Biosens. Bioelectron.* **2009**, *24*, 2654−2658.
(64) Batalla, P.; Fuentes, M.; Mateo, C.; Grazu, V.; Fernandez-Lafuente, R.; Guisan, J. M. *Biomacromolecules* **2008**, *9*, 2230−2236.
(65) Trmcic-Cvitas, J.; Hasan, E.; Ramstedt, M.; Li, X.; Cooper, M. A.; Abell, C.; Huck, W. T. S.; Gautrot, J. E. *Biomacromolecules* **2009**, *10*, 2885−2894.
(66) Goto, Y.; Matsuno, R.; Konno, T.; Takai, M.; Ishihara, K. *Biomacromolecules* **2008**, *9*, 828−833.